ON MIXTURES AS WORKING FLUIDS FOR AIR-COOLED ORC BOTTOMING POWER PLANTS OF GAS TURBINES

Dabo Krempus[1]*, Sebastian Bahamonde[1], Teus van der Stelt[2], Carlo M. De Servi[1,3], Wolfgang Klink[4], Piero Colonna[1]

[1]Propulsion and Power, Delft University of Technology, The Netherlands
[2]Asimptote bv, Heeswijk-Dinther, The Netherlands
[3]VITO, Thermal Energy Systems, Mol, Belgium
[4]Siemens Energy AG, Erlangen, Germany
*Corresponding Author: d.krempus@tudelft.nl

ABSTRACT

The use of mixtures as working fluids of organic Rankine cycle (ORC) waste heat recovery (WHR) power plants has been proposed in the past to improve the matching between the temperature profile of the hot and the cold streams of condensers and evaporators, and the possible increase in thermodynamic efficiency of the system. The goal of this study was to assess the benefits in terms of efficiency, environmental (GWP) and operational safety (flammability) that can be obtained by selecting binary mixtures as working fluids in air-cooled ORC bottoming power plants of medium-capacity industrial gas turbines. Furthermore, two thermodynamic cycle configurations were analyzed, namely the simple and the split-cycle configuration. The benchmark case is a combined cycle power plant formed by an industrial gas turbine and an air-cooled recuperated ORC power unit with cyclopentane as the working fluid. The results of this study indicate that binary mixtures provide the designer with a wider choice of optimal working fluids, however, in the case of the simple-cycle configuration, the improvement in terms of combined cycle efficiency over the benchmark case is rather limited. The so-called split-cycle configuration leads to a general performance enhancement especially in combination with working fluid blends. Furthermore, this cycle configuration enables the use of environmentally and operationally safe working fluids if compared to cyclopentane, with no penalty in terms of combined cycle efficiency.

1 INTRODUCTION

Mixtures are an interesting option as working fluids for air-cooled recuperated ORC WHR systems of medium-capacity stationary gas turbines. Nowadays, such applications demand high combined cycle efficiency as well as compatibility with regulations regarding the environmental and operational safety of working fluids. The research documented here aimed at evaluating whether these requirements could be better met with working fluid mixtures instead of the pure fluids which are currently used.
The exploitation of the mixture temperature glide in the condenser and in the evaporator is of special interest for energy conversion systems entailing heat transfer with a gas and benefiting from a reduction of its mass flow. For example, the efficiency of air-cooled ORC power plants might benefit from non-isothermal condensation because air-cooler fan power can be reduced in comparison to the air-cooler fan power needed for the isothermal condensation of a pure working fluid. However, more heat transfer surface is required. In their work on mixtures as working fluids for air-cooled ORC WHR systems for fuel cells, Angelino and Colonna (2000) showed that the improved temperature profile matching in the condenser, due to the working fluid temperature glide, leads to a reduction of air-cooler fan power and may contribute to an increase of the combined cycle net power output. Bramaikis *et al.* (2020) investigated the use of binary mixtures made of low GWP refrigerants for generic superheated WHR water-cooled ORC systems. They concluded that, for the considered working fluid mixtures, the net power output by adopting blends is never larger than that resulting from using pure fluids, even if the amount of recovered thermal energy might be larger. The presented work is a first step towards the

final goal of filling the knowledge gap regarding the use of working fluid mixtures in high temperature WHR air-cooled ORC power plants. The impact of using mixtures on combined cycle efficiency, especially considering its influence on air-cooler fan power demand, as well as the potential of finding environmentally and operationally safer fluids is analyzed.

2 METHODOLOGY

2.1 Thermodynamic Cycle Configurations

Two cycle configurations were considered in this study. With reference to Figure 1, these are the simple recuperated cycle and the novel split-cycle (Gaia *et al.*, 2017). Both cycles use an air-cooled condenser (Cond). In the split-cycle, the flow is divided into two streams downstream of the pump. One stream passes through the recuperator (Rec) while the other one exchanges heat with the heat source in the preheater (Pre). Both streams are merged before entering the heat recovery steam generator (HRSG). The degree of mass flow split m_{frac} is defined as the fraction of recuperator cold side over hot side mass flow rate.

The benchmark case is a power plant using a Siemens SGT-750 gas turbine equipped with an ORC WHR system. This system implements the simple-cycle configuration and uses cyclopentane as the working fluid. The gas turbine has a nominal power output $\dot{W}_{\mathrm{GT}}$ of 34.6 MW and an efficiency η_{GT} of 38.5% at an ambient temperature T_{amb} of 30°C. The ORC power plant net power output $\dot{W}_{\mathrm{net}}$ is 9.9 MW. This results in a combined cycle power output of 44.5 MW and a combined cycle efficiency η_{CC} of 49.5%, with $\eta_{\mathrm{CC}} = \frac{\dot{W}_{\mathrm{GT}}+\dot{W}_{\mathrm{net}}}{\frac{\dot{W}_{\mathrm{GT}}}{\eta_{\mathrm{GT}}}}$.

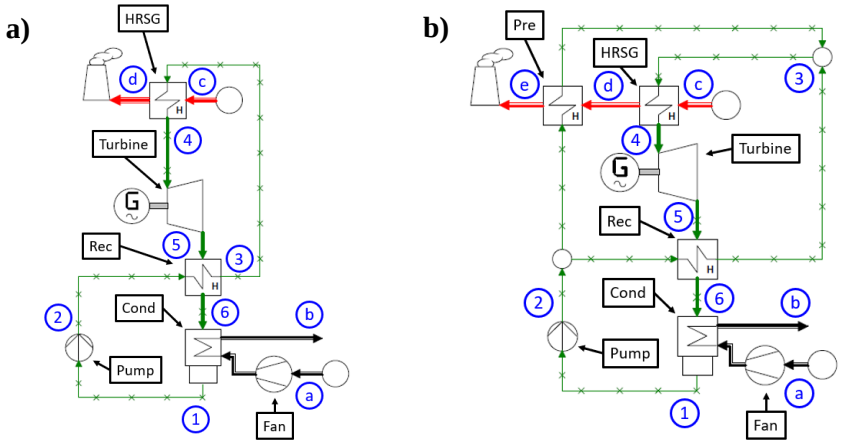

Figure 1: Process flow diagrams of simple-cycle a) and split-cycle b) configuration

2.2 Thermodynamic Cycle Specifications

Table 1 indicates the general cycle specifications. The following constraints were applied:

- superatmospheric condensing pressure, i.e., minimum cycle pressure $\geq 1.01325\ 10^5$ Pa;
- cycle maximum temperature limited by working fluid thermal stability.

The superatmospheric condensing pressure constraint is applied to prevent leakage of ambient air into the system. Avoiding air leakage has two operational reasons: First, in case a flammable working fluid is used, leaked air can lead to the formation of an ignitable mixture inside the system which poses a safety issue. Second, oxygen is a catalyst for thermal decomposition of the working fluid which reduces fluid lifetime and plant performance. In case of a cycle with subatmospheric condensing pressure it is necessary to adopt a deaerator to cope with the preceding issues. This component introduces additional cost and can affect the reliability of the plant. Solutions that did not fulfill the superatmospheric pressure constraint were discarded. The second constraint was ensured by setting an upper bound to the maximum cycle temperature.

Table 1: Thermodynamic cycle specifications

Parameter	Value	Parameter	Value
$T_{\mathrm{HRSG_{H_{in}}}}$*	760.25 K	$\Delta T_{\mathrm{pp_{Rec}}}$	10 K
$\dot{m}_{\mathrm{HRSG}}$*	105.6 kg/s	$\Delta p_{\mathrm{Rec_H}}$	5000 Pa
$\Delta p_{\mathrm{HRSG_H}}$*	2500 Pa	$\Delta p_{\mathrm{Rec_C}}$	2.5% of $p_{\max}$
$\Delta p_{\mathrm{HRSG_C}}$	2.5% of $p_{\max}$	Δp_{Pre} **	0 Pa
$\Delta T_{\mathrm{pp_{HRSG}}}$	10 K	η_{pump}	70%
$\Delta T_{\mathrm{pp_{Cond}}}$*	7 K	η_{turbine}	80%
$\Delta p_{\mathrm{Cond_H}}$	5000 Pa	η_{fan}	75%
$\Delta p_{\mathrm{Cond_C}}$	200 Pa	T_{amb}*	303.15 K

** Values provided by Klink (2018). Remaining values are estimates.*
*** Entire pressure drop assumed in HRSG.*

Table 2: Simulation cases and settings

Simulation Case*	Optimization variables
pure/simple	$T_{\min}$, $T_{\max}$, $p_{\max}$
pure/split	$T_{\min}$, $T_{\max}$, $p_{\max}$, m_{frac}
binary/simple	$T_{\min}$, $T_{\max}$, $p_{\max}$, z_{i}
binary/split	$T_{\min}$, $T_{\max}$, $p_{\max}$, z_{i}, m_{frac}

** Working fluid composition/cycle configuration*

Table 3: List of candidate fluids

	Synonym	Chemical Formula	CAS-Nr.	P_{crit} (10^5Pa)	T_{crit} (K)	Molecular Weight (kg/kmol)	T_{limit} (K)	T_{NBP} (K)	GWP	Flamm-ability
Old Refrig.	R125	C2HF5	354-33-6	36.2[a]	339.2[a]	120.0[a]	669[b]	225[a]	3500[c]	No[c]
	R134a	C2H2F4	811-97-2	40.6[a]	374.2[a]	102.0[a]	641[b]	247[a]	1300[d]	No[d]
	R32	CH2F2	75-10-5	57.8[a]	351.3[a]	52.0[a]	843[c]	221[a]	675[c]	Mild[c]
	R245fa	C3H3F5	460-73-1	36.4[a]	427.2[a]	134.0[a]	573[s]	288[a]	858[f]	No[d]
Modern Refrig.	HFO-1336mzz-Z	C4H2F6	692-49-9	30.5[d]	444.30[d]	164.1[d]	523[e]	306[d]	2[d]	No[d]
	HFO-1336mzz-E	C4H2F6	66711-86-2	32.9[d]	412.5[d]	164.1[d]	523[g]	281[d]	18[d]	No[d]
	HCFO-1224yd-Z	C3HClF4	111512-60-8	33.8[d]	429.2[d]	148.5[d]	448[f,*]	287[d]	1[d]	No[d]
	HCFO-1233zd-E	C3H2ClF3	102687-65-0	36.2[d]	439.7[d]	130.5[d]	450[k,*]	291[d]	7[k]	No[d]
	HFO-1234yf	C3H2F4	754-12-1	33.8[a]	367.9[a]	114.0[a]	N/A[*]	244[a]	4[h]	Mild[l]
	HFO-1243zf	C3H3F3	677-21-4	36.1[a]	378.6[a]	96.1[a]	N/A[*]	248[a]	0.8[h]	Mild[l]
	Novec 649	C6F12O	756-13-8	18.7[n]	441.8[n]	316.0[i]	573[i]	322[i]	1[i]	No[i]
HCs	cyclopentane	C5H10	287-92-3	45.1[a]	511.7[a]	70.1[a]	573[c]	322[a]	6[c]	Yes[c]
	toluene	C7H8	108-88-3	41.1[a]	591.8[a]	92.1[a]	673[c]	384[a]	3.3[o]	Yes[c]
	isobutane	C4H10	75-28-5	36.4[a]	407.8[a]	58.1[a]	593[q]	261[a]	3[d]	Yes[d]
	propane	C3H8	74-98-6	42.5[a]	369.8[a]	44.1[a]	633[r]	231[a]	3[d,o]	Yes[d]
	ethane	C2H6	74-84-0	48.7[a]	305.3[a]	30.1[a]	633[r]	185[a]	2.9[o]	Yes
Siloxanes	D4	C8H24O4Si4	556-67-2	13.2[a]	586.5[a]	296.6[a]	623[c]	448[a]	0[c]	Mild[c]
	D5	C10H30O5Si5	541-02-6	10.4[a]	617.4[a]	370.8[a]	623[c]	484[a]	0[c]	Mild[c]
	D6	C12H36O6Si6	540-97-6	9.01[a]	645.8[a]	444.9[a]	623[c]	518[a]	0[c]	Mild[c]
	MM	C6H18OSi2	107-46-0	19.2[a]	519.0[a]	162.4[a]	573[c]	374[a]	0[c]	Yes[c]
	MDM	C8H24O2Si3	107-51-7	14.6[a]	564.4[a]	236.5[a]	573[c]	426[a]	0[c]	Mild[c]
	MD2M	C10H30O3Si4	141-62-8	11.9[a]	599.4[a]	310.7[a]	573[c]	477[a]	0[c]	Mild[c]
	MD3M	C12H36O4Si5	141-63-9	9.45[a]	628.4[a]	384.8[a]	573[c]	503[a]	0[c]	Mild[c]
	MD4M	C14H42O5Si6	107-52-8	8.04[a]	653.2[a]	459.0[a]	573[c]	533[a]	0[c]	Mild[c]
PFCs	PP2	C7F14	355-02-2	20.2[m]	486.4[m]	350.1[m]	673[l]	349[m]	N/A[$]	No[l]
	PP5	C10F18	306-94-5	17.8[m]	565.1[m]	462.1[m]	673[l]	415[m]	7190[p]	No[l]

[a] Rowley *et al.* (2006), using 2019 Database
[b] Calderazzi and Colonna (1997)
[c] Astolfi and Macchi (2017)
[d] Arpagaus *et al.* (2018)
[e] Kontomaris (2014)
[f] Mateu-Royo *et al.* (2019)
[g] Juhasz (2017)
[h] McLinden *et al.* (2014)
[i] 3M Corp. (2009)
[j] Takizawa *et al.* (2009)
[k] Perkins and Huber (2017)
[l] F2 Chemicals Ltd. (2012)
[m] Marsh *et al.* (2007)
[n] McLinden *et al.* (2015)
[o] Collins *et al.* (2002)
[p] IPCC (2013)
[q] Dai *et al.* (2016)
[r] Acc. to Preißinger *et al.* (2016) the compound is present as decomposition product of MM at T > 633.15K
[s] Angelino and Invernizzi (2003)
[*] For this analysis 523 K was assumed
[$] Assumed to be same as for PP5

2.3 Candidate Fluids

The fluids selected for this analysis comprehend fluids featuring high thermal stability (HCs, PFCs, Siloxanes), low GWP and low flammability (HFC, HFOs, HCFOs). These are listed in Table 3 together with their main characteristics. The ozone depletion potential of all fluids except for the fluids HCFO-1244yd-Z and HCFO-1233zd-E is zero. For the latter two Arpagaus *et al.* (2018) state values of 1.2E-4 and 3.4E-4, respectively.

2.4 Thermodynamic Models

The analysis was conducted using in-house tools for thermodynamic cycle calculations (Bahamonde, 2019) and fluid property modeling (Colonna *et al.*, 2019). The PCP-SAFT equation of state was used in this study. Due to lack of experimental data all mixture binary interaction parameters were set to zero. Therefore, despite the predictive capabilities of PCP-SAFT uncertainties in the results can be expected. The optimum cycle parameters and the optimal mixture composition (z_{i}) were found by using the evolutionary algorithm *eaMuPlusLambda* implemented in the Python library DEAP (Fortin *et al.*,

2012). The optimization objective was $\dot{W}_{\mathrm{net}}$ and the optimization variables were cycle minimum temperature T_{min}, cycle maximum temperature T_{max}, cycle maximum pressure p_{max}, z_{i} and m_{frac}. For mixtures, the upper bound of T_{max} was set equal to the lowest thermal stability limit of the involved compounds. The upper bound of p_{max} was set to 1.2 times the critical pressure of the fluid. Higher cycle pressures offer limited benefits in terms of cycle efficiency due to the increased pump power demand. High pump power demand also leads to an increased sensitivity of cycle efficiency to pump isentropic efficiency. Consequently, higher cycle pressure leads to increased component complexity and cost. For example, as opposed to the off-the-shelf pumps commonly used for subcritical ORC systems, a multi-stage pump is required for supercritical cycles. Furthermore, the primary heat exchanger walls need to be thicker to sustain higher pressure (Astolfi and Macchi, 2017). Air-cooler fan power consumption $\dot{W}_{\mathrm{fan}}$ is calculated as the product of cooling air mass flow rate $\dot{m}_{\mathrm{Cond_C}}$ times condenser cold side pressure drop $\Delta p_{\mathrm{Cond_C}}$ divided by air density and fan isentropic efficiency. For the same amount of rejected thermal power, a temperature glide over condensation allows for an increased heating of the cooling air and thus a reduction in $\dot{m}_{\mathrm{Cond_C}}$. As $\Delta p_{\mathrm{Cond_C}}$ is fixed (see in Table 1), only the impact of the $\dot{m}_{\mathrm{Cond_C}}$ variation on $\dot{W}_{\mathrm{fan}}$ is accounted for in this analysis. The gas turbine exhaust gas was modelled as an ideal gas mixture with a molar composition of 73.9% N_2, 13.8% O_2, 3.1% CO_2, 8.1% H_2O and 0.9% Ar (Klink, 2018).

3 RESULTS

325 binary mixtures resulting from the combination of the fluids in Table 3 were assessed. The performance of cycles employing binary mixtures was compared against that achievable with cycles employing pure working fluids. All simulations were run based on the cycle specifications listed in Table 1 and the optimization settings given in Table 2. Only cases that fulfilled the constraint of superatmospheric condensing pressure are presented hereafter.

Figure 2 shows a comparison between the simple-cycle and split-cycle in the temperature entropy diagram of R245fa as an example. Both cycles are super-critical and feature a similar minimum and maximum temperature. The maximum temperatures are close to the estimated thermal stability limit of the working fluid, which is 573 K. The split-cycle allows to recover substantially more thermal energy from the exhaust gases due to the preheater. The combined cycle efficiency increases by about 3%. However, such a large performance increase is not obtained for all fluids and depends on the fluid's critical temperature T_{crit} as discussed in Chapter 4.

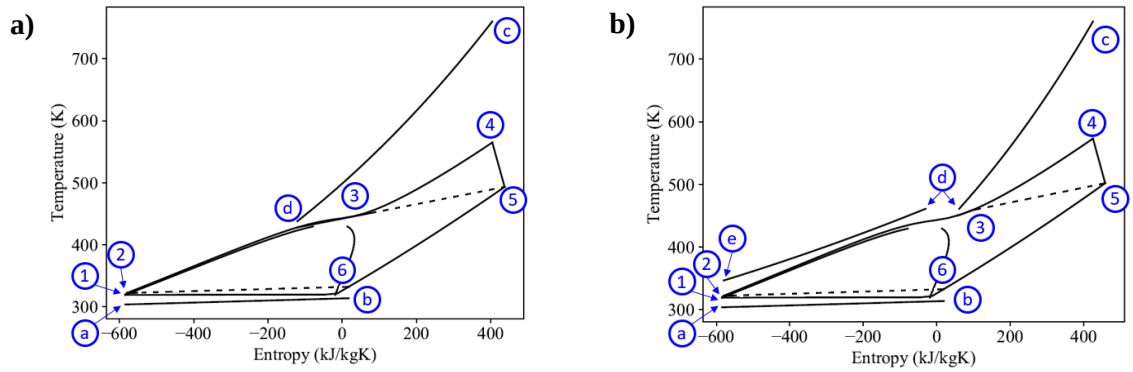

Figure 2: Ts-diagram for simple-cycle a) and split-cycle b) configuration using R245fa; station numbering according to Figure 1; Note 1: dashed lines indicate heat transfer between hot and cold recuperator streams; Note 2: gap in saturation curve close to the critical point is due to modelling difficulties of the PCP-SAFT equation of state very close to this region

Figure 3 presents $\dot{W}_{\mathrm{net}}$ as a function of T_{crit} and molecular complexity for the simple-cycle and split-cycle. Molecular complexity is defined according to Angelino *et al.* (1991). Note that the T_{crit} values are calculated as prescribed by the PCP-SAFT model and therefore might differ from experimental

values. Higher power output can be achieved with the split-cycle as compared to the simple-cycle. Furthermore, the best performance can be obtained with the split-cycle and fluids with lower T_{crit}.

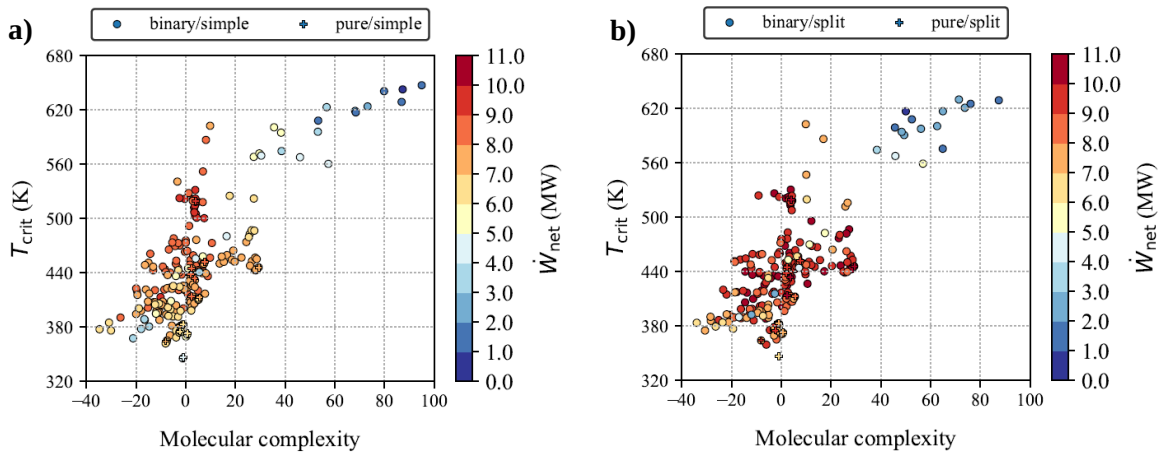

Figure 3: $\dot{W}_{\mathrm{net}}$ as function of T_{crit} and molecular complexity for both the simple-cycle a) and the split-cycle b)

Figure 4 presents η_{CC} in relation to a representative selection of fluids. The corresponding working fluid composition is indicated in Table 4. Non-flammable fluids with a GWP ≤ 150 are highlighted in blue in Figure 4. The results show that the split-cycle configuration leads to a better performance for all fluids and can also outperform the benchmark cycle. Furthermore, some low GWP/non-flammable fluids achieve a performance comparable to that of the benchmark if the split-cycle configuration is adopted.

For the simple-cycle with a pure working fluid, cyclopentane provides the best performance. However, for the split-cycle configuration R245fa performs best followed by isobutane and cyclopentane.

Mixtures offer a wider range of fluids whose use provides good combined cycle performance, but, as for the simple-cycle configuration, the benchmark provides the best performance. Only in the case of the split-cycle configuration, the use of a mixture is beneficial if compared to a pure fluid, including cyclopentane. Despite the large variety of mixtures, in case of the simple-cycle configuration, 19 of the 20 mixtures providing the best η_{cc} contain cyclopentane with mole fraction above 90%. Furthermore, among the 100 mixtures providing the best η_{cc} 10 feature a low GWP and are non-flammable in case of the simple-cycle and 13 in case of the split-cycle.

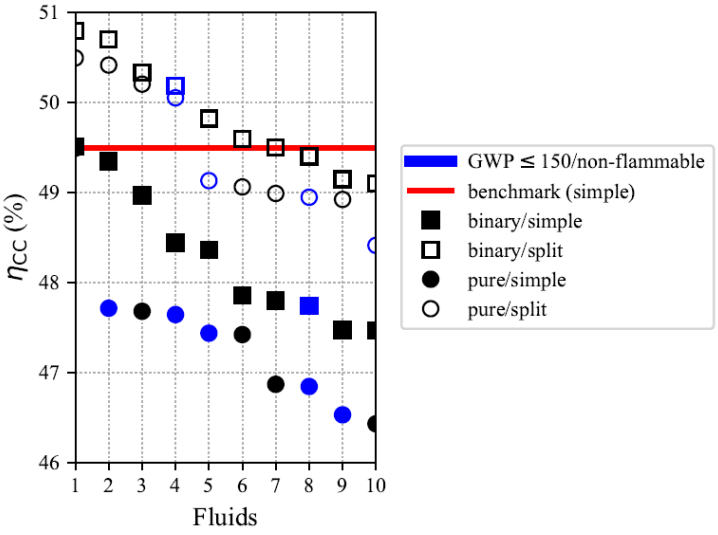

Figure 4: η_{CC} for a selection of fluids. Fluid number identifier in Table 4.

Table 4: Table of selected fluids

Fluid	pure/simple	pure/split	binary/simple	binary/split
1	Cyclopentane	R245fa	Cyclopentane[0.92]& R134a[0.08]	R245fa[0.72]& PP2[0.28]
2	HFO-1233zd-Z*	Isobutane	Cyclopentane[0.79]& R245fa[0.21]	R245fa[0.68]& Cyclopentane[0.32]
3	R245fa	Cyclopentane	Cyclopentane[0.80]& HFO-1336mzz-Z[0.20]	Cyclopentane[0.93]& Isobutane[0.07]
4	HFO-1336mzz-Z*	Novec 649*	R245fa[0.94]& D5[0.06]	Novec 649[0.95]& R134a[0.05]*
5	HCFO-1224yd-Z*	HFO-1336mzz-Z*	HCFO-1233zd-E[0.83]& Toluene[0.17]	R32[0.83]& Toluene[0.17]
6	Isobutane	R134a	HCFO-1224yd-Z[0.90]& MM[0.10]	HFO-1336mzz-Z[0.92]& HFO-1243zf[0.08]
7	R32	HCFO-1224yd-Z*	Isobutane[0.73]& R32[0.27]	Propane[0.89]& D4[0.11]
8	Novec 649*	R32	HCFO-1233zd-E[0.61]& HFO-1336mzz-Z[0.39]*	Novec 649[0.85]& MM[0.15]
9	HFO-1336mzz-E*	HCFO-1233zd-Z*	Isobutane[0.80]&Novec 649[0.20]	HCFO-1233zd-E[0.78]& R134a[0.22]
10	R134a	HFO-1336mzz-E*	HCFO-1224yd-Z[0.94]& HFO-1243zf[0.06]	HCFO-1224yd-Z[0.76]& Isobutane[0.24]

***** Fluids with GWP $\leq$ 150 and zero flammability

4 DISCUSSION

4.1 Relation between Cycle Configuration and Fluid Critical Temperature

Figure 5 shows η_{CC} with respect to T_{crit} for both the simple-cycle and split-cycle configurations. In case of the split-cycle configuration, η_{CC} reaches the highest values for T_{crit} that are approximately 100 K lower than the T_{crit} of the fluids providing the best performance in case of the simple-cycle configuration.

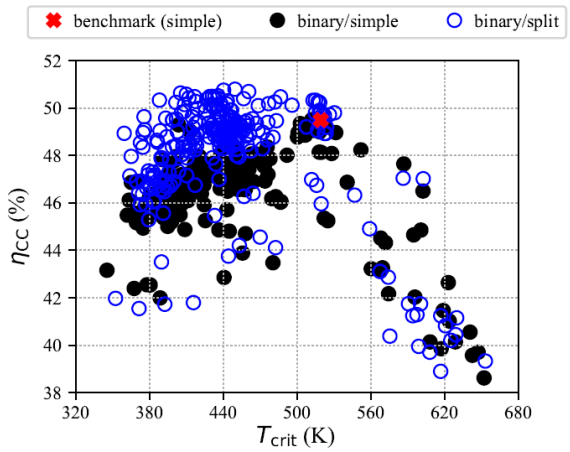

Figure 5: Comparison of η_{CC} over T_{crit}

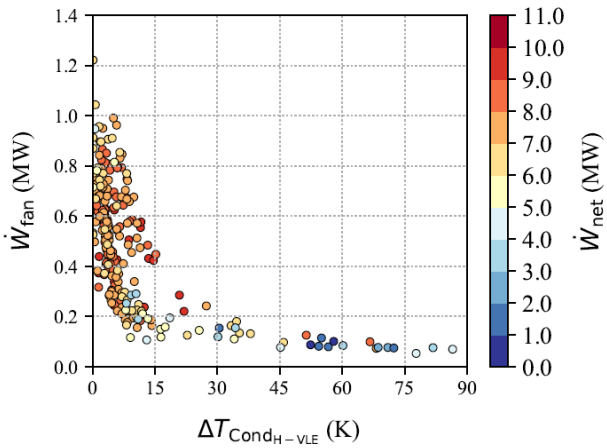

Figure 6: $\dot{W}_{net}$ as a function of $\dot{W}_{fan}$ and $\Delta T_{Cond_{H-VLE}}$ for the binary/simple case

4.2 Effect of Temperature Glide

The isobaric phase change of a zeotropic mixture is non-isothermal, therefore it occurs with a temperature glide. This physical behavior is beneficial for the temperature profile matching in the condenser and in the evaporator. The analysis of this specific application shows that the temperature glide does not substantially influence the average temperature at which thermal energy is discharged as compared to a cycle using a pure fluid. Since most optimum cycle designs identified in this work are of the super-critical type, evaporation is not affected the temperature glide. Nevertheless, the majority of investigated binary mixtures result in lower average temperature at which thermal energy is added. This results in reduced thermodynamic efficiency for cycles employing binary mixtures. However, the temperature glide in the condenser can help to increase $\dot{W}_{net}$ of air-cooled ORC systems by reducing $\dot{W}_{fan}$. Figure 6 shows $\dot{W}_{net}$ as a function of $\dot{W}_{fan}$ and condenser temperature glide occurring across the vapor-liquid equilibrium (VLE) region $\Delta T_{Cond_{H-VLE}}$ for the simple-cycle. $\dot{W}_{fan}$ reduces for increasing

values of the $\Delta T_{\mathrm{Cond_{H-VLE}}}$. High values of $\dot{W}_{\mathrm{net}}$ are however only obtained for a narrow range of low $\Delta T_{\mathrm{Cond_{H-VLE}}}$ values. Outside this range the beneficial $\dot{W}_{\mathrm{fan}}$ reduction is offset by the decrease in thermodynamic efficiency mentioned above. Figure 7 shows $\Delta T_{\mathrm{Cond_{H-VLE}}}$ for the selected fluids given in Table 4.

4.3 Working Fluid and Turbine Design

Turbine design, size and therefore cost, is driven by the specific enthalpy difference $\Delta h_{\mathrm{turbine}}$ and the volume flow ratio VR (Astolfi and Macchi, 2017). Figure 9 displays the variation of these parameters for pure fluids and binary mixtures. With the simple-cycle configuration, the highest η_{cc} is achieved with fluids featuring high $\Delta h_{\mathrm{turbine}}$ and VR. These fluids contain a large mole fraction of cyclopentane. On the other hand, with the split-cycle, high η_{cc} is obtained with fluids featuring lower $\Delta h_{\mathrm{turbine}}$ and VR. For example, Figure 9b indicates that high performance can be attained with fluids leading to a VR range from 10 to 25 and a $\Delta h_{\mathrm{turbine}}$ between 30 and 60 kJ/kg. Comparing this VR range with the data given in Figure 8 and Table 4 reveals that mixtures in this region are based on R245fa and modern refrigerants. Modern refrigerants are characterized by very low GWP and zero flammability. Of special interest could be the low GWP and non-flammable fluid Novec 649. This fluid used in the split-cycle configuration entails η_{cc} higher than that of the benchmark, a VR of 23.6 and $\Delta h_{\mathrm{turbine}}$ of 32.7 kJ/kg. Such a fluid would fulfill regulations concerning environmental and operational safety as well as result in a compact and cheap turbine design.

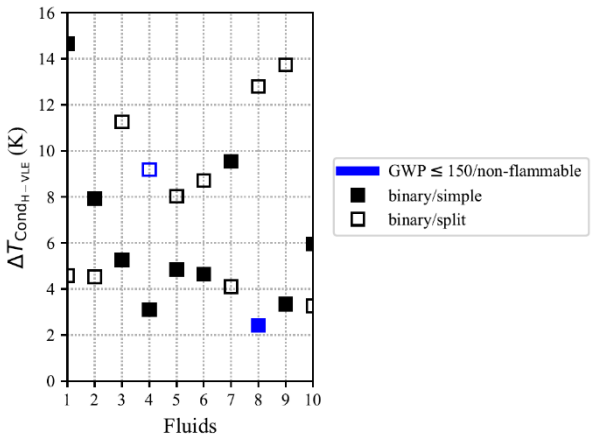

Figure 7: $\Delta T_{Cond_{H-VLE}}$ for selected fluids. Fluid number identifier in Table 4.

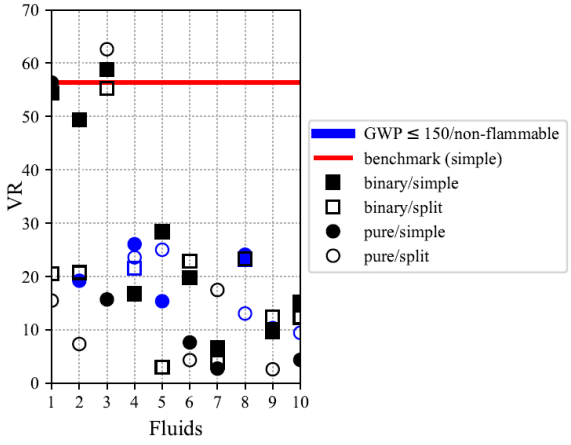

Figure 8: VR for selected fluids. Fluid number identifier in Table 4.

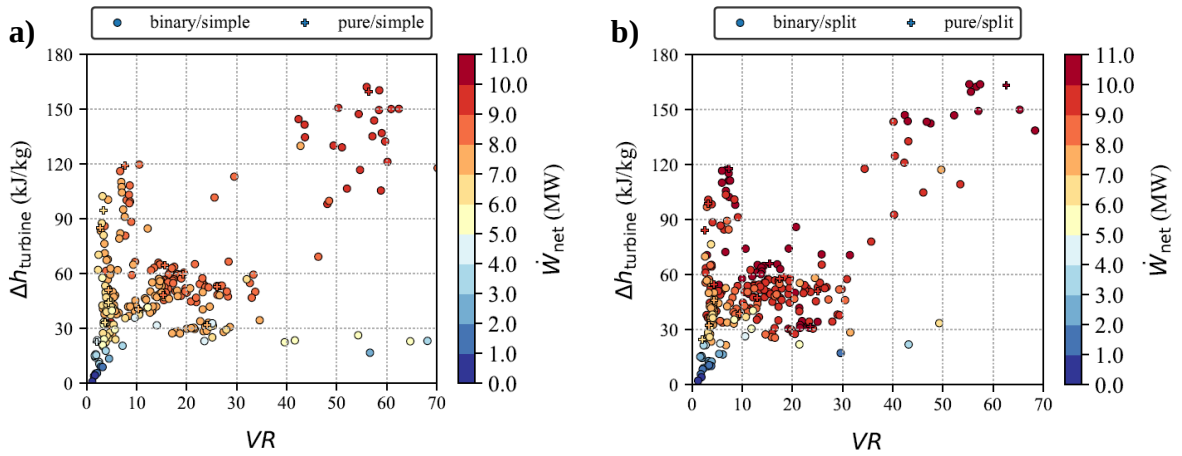

Figure 9: $\dot{W}_{\mathrm{net}}$ as a function of $\Delta h_{\mathrm{turbine}}$ and VR for the simple-cycle a) and split-cycle b)

5 CONCLUSION

The use of mixtures as working fluids for air-cooled ORC systems as bottoming cycle of medium-capacity gas turbines was investigated by means of steady state simulations. Zeotropic mixtures undergo isobaric phase change with a temperature glide, and this effect can in principle be exploited to reduce condenser fan power consumption at the cost of additional heat transfer surface. As a result, overall combined cycle efficiency may increase. Low GWP and non-flammable fluids suitable for high temperature waste heat recovery were considered in this study. Furthermore, a new cycle configuration especially suitable for waste heat recovery was conceived and tested as a part of this study. The main findings are:

- In comparison to pure fluids, a larger number of mixtures can be used as working fluids of high-performance air-cooled ORC systems. However, even if the benefit of air-cooler fan power reduction was verified, under the given assumptions the performance of the benchmark case employing cyclopentane as the working fluid could not be overcome, due to the lower equivalent thermodynamic temperature of evaporation in case of a mixture as the working fluid.
- The split-cycle configuration allows to increase the combined cycle efficiency if compared to the simple recuperated cycle configuration and the performance estimated with a wide range of working fluids is better than the performance calculated for the benchmark. The optimum combined cycle performance is achieved with fluids featuring lower critical temperature as compared with the working fluids of the simple recuperated cycle configuration.
- A range of pure fluids and mixtures allow to design a more compact and thus cheaper turbine if compared to the turbine of the benchmark case.
- The combined cycle efficiency of a system adopting the split-cycle configuration for the bottoming unit and Novec 649 as the working fluid, a low GWP and non-flammable fluid, is higher than the efficiency computed for the benchmark case.

The performance improvement achieved with the split-cycle configuration comes at the cost of larger heat exchanger surfaces. In order to quantify the advantage of this configuration, the economic aspects related to the need of more heat transfer surface and turbine design need to be taken into account. As a last remark, it must be noted that, while the PCP-SAFT equation of state employed in this study to calculate the thermodynamic properties of fluids belongs to the class of physics-based models, its application to highly non-ideal mixtures without a proper estimation of binary interaction parameters introduces substantial uncertainties.

NOMENCLATURE

η	isentropic efficiency	(-)	**Subscript**	
GWP	global warming potential over 100 years	(-)	C	cold side fluid
$\dot{m}$	mass flow rate	(kg/s)	crit	critical point
p	pressure	(Pa)	H	hot side fluid
T	temperature	(K)	in	inflowing
T_{limit}	thermal stability limit of fluid	(K)	pp	pinch point
T_{NBP}	normal boiling point of fluid	(K)		

REFERENCES

Angelino, G., Colonna, P., 2000, Air Cooled Siloxane Bottoming Cycle for Molten Carbonate Fuel Cells, *Fuel Cell Seminar*: p. 667-670.

Angelino, G., Invernizzi, C., Macchi, E., 1991, Organic Working Fluid Optimization for Space Power Cycles, *In:* Angelino, G., De Luca, L., Sirignano, W. A., *Modern Research Topics in Aerospace Propulsion*, Springer, New York, NY, USA: p. 297-326.

Angelino, G., Invernizzi, C., 2003, Experimental Investigation on the Thermal Stability of Some New Zero ODP Refrigerants, *Int. J. Refrig.*, vol. 26, no. 1: p. 51-58.

Arpagaus, C., Bless, F., Uhlmann, M., Schiffmann, J., Bertsch, S., 2018, High Temperature Heat Pumps: Market Overview, State of the Art, Research Status, Refrigerants, and Application Potentials, *Energy*, vol. 152: p.985-1010.

Astolfi, M., Macchi, E., 2017, *Organic Rankine Cycle (ORC) Power Systems*, Woodhead Publishing, Cambridge, United Kingdom: 665 p.

Bahamonde, S., 2019, Pycle: Program for Thermodynamic Cycle Calculations, [computer program].

Braimakis, K., Mikelis, A., Charalampidis, A., Karellas, S., 2020, Exergetic Performance of CO2 and Ultra-low GWP Refrigerant Mixtures as Working Fluids in ORC for Waste Heat Recovery, *Energy*, vol. 203: 23 p.

Calderazzi, L., Colonna, P., 1997, Thermal Stability of R-134a, R-141b, R-1311, R-7146, R-125 Associated with Stainless Steel as a Containing Material, *Int. J. Refrig.*, vol. 20, no. 6: p. 381-389.

Collins, W.J., Derwent, R.G., Johnson, C.E, Stevenson, D.S., 2002, The Oxidation of Organic Compounds in the Troposphere and their Global Warming Potentials, *Climatic Change*, vol. 52: p. 453–479.

Colonna, P., van der Stelt, T.P., Guardone, A., 2019, FluidProp (Version 3.1): A program for the estimation of thermophysical properties of fluids, [computer program].

Dai, X., Shi, L., An, Q., Qian, W., 2016, Screening of Hydrocarbons as Supercritical ORCs Working Fluids by Thermal Stability, *Energy Conversion and Management*, vol. 125: p. 632-637.

Fortin, F., De Rainville, F., Gardner, M., Parizeau, M., Gagné, C., 2012, DEAP: Evolutionary Algorithms Made Easy, *J. Machine Learning Research*, vol. 20: p. 2171-2175.

F2 Chemicals Ltd., 2012, Product Datasheet, online: https://f2chemicals.com/pdf/technical/Compatability.pdf, last accessed 28th April 2021.

Gaia, M., Bini, R., Vescovo, R., Spagnoli, E., 2017, Cogenerative Organic Rankine Cycle System, Patent no.: WO 2017/199170 Al, assigned to: Turboden S.P.A.

IPCC, 2013, *Climate Change 2013: The Physical Science Basis. Contribution of Working Group I to the Fifth Assessment Report of the Intergovernmental Panel on Climate Change*, Cambridge University Press, Cambridge, United Kingdom and New York, NY, USA, 1535 p.

Juhasz, J.R., 2017, Novel Working Fluid, HFO-1336mzz(E), for Use in Waste Heat Recovery Application, *IEA Heat Pump Conference*: 10 p.

Klink, W., 2018, Personal Communication with Wolfgang Klink of Siemens Energy AG.

Kontomaris, K., 2014, HFO-1336mzz-Z: High Temperature Chemical Stability and Use as a Working Fluid in Organic Rankine Cycles, *Int. Refrig. and Air Cond. Conference*: 10 p.

Marsh, K.N., Abramson, A., Ambrose, D., Morton, D.W., Nikitin, E., Tsonopoulos, C., Young, C. L., 2007, Vapor-liquid Critical Properties of Elements and Compounds. 10. Organic Compounds Containing Halogens, *J. Chem. Eng. Data*, vol. 52, no. 5: p. 1509-1538.

Mateu-Royo, C., Navarro-Esbrí, J., Mota-Babiloni, A., Amat-Albuixech, M., Molés, F., 2019, Thermodynamic Analysis of Low GWP Alternatives to HFC-245fa in High-temperature Heat Pumps: HCFO-1224yd(Z), HCFO-1233zd(E) and HFO-1336mzz(Z), *Applied Thermal Engineering*, vol. 152: p. 762-777.

McLinden, M.O., Kazakov, A.F., Brown, J.S., Domanski, P.A., 2014, A Thermodynamic Analysis of Refrigerants: Possibilities and Tradeoffs for Low-GWP Refrigerants, *Int. J. Refrig.*, vol. 38: p. 80-92.

McLinden, M.O., Perkins, R.A., Lemmon, E.W., Fortin, T.J., 2015, Thermodynamic Properties of 1,1,1,2,2,4,5,5,5-Nonafluoro-4-(trifluoromethyl)-3-pentanone: Vapor Pressure, (p, ρ, T) behavior,

and Speed of Sound Measurements, and an Equation of State, *J. Chem. Eng. Data*, vol. 60, no. 12: p. 3646-3659.

Perkins, R.A., Huber, M.L., 2017, Measurement and Correlation of the Thermal Conductivity of trans-1-Chloro-3,3,3-trifluoropropene (R1233zd(E)), *J. Chem. Eng. Data*, vol. 62, no. 9: p. 2659-2665.

Preißinger, M., Brüggemann, D., 2016, Thermal Stability of Hexamethyldisiloxane (MM) for High-temperature Organic Rankine Cycle (ORC), *Energies*, vol. 9, no. 3: 11 p.

Rowley, R., Widling, W., Oscarson, J., Yang, Y., Zundel, N., Daubert, T., Danner, R., 2006, DIPPR®Data Compilation of Pure Chemical Properties, Design Institute for Physical Properties, AIChE, New York, NY, USA.

Takizawa, K., Tokuhashi, K., Kondo, S., 2009, Flammability Assessment of CH_2=$CFCF_3$: Comparison with Fluoroalkenes and Fluoroalkanes, *J. Hazardous Materials*, vol. 172: p. 1329-1338.

3M Corporation, 2009, Novec™ 649 Product Datasheet, online: https://multimedia.3m.com/mws/media/569865O/3m-novec-engineered-fluid-649.pdf, last accessed 28th April 2021.